C. R. Mecanique 339 (2011) 250–256

Contents lists available at ScienceDirect

Comptes Rendus Mecanique

www.sciencedirect.com

Unstable modes of laminar round fountains on inclined wall

Modes instables de fontaines circulaires laminaires sur parois inclinées

Aymeric Lamorlette *, Rabah Mehaddi, Olivier Vauquelin

IUSTI (UMR CNRS 6595), Aix-Marseille université, technopôle de Château-Gombert, 60, rue Joliot Curie, 13453 Marseille cedex 13, France

ARTICLE INFO

Article history:
Received 10 January 2011
Accepted 26 January 2011
Available online 2 March 2011

Keywords:
Fluid mechanics
Laminar fountain
Unstable modes
Inclined wall

Mots-clés :
Mécanique des fluides
Fontaine laminaire
Modes instables
Paroi inclinée

ABSTRACT

Experiments were carried out on reversed weak laminar inclined fountains to asses that unstable modes of round fountains are disturbed by the inclination. Indeed, compared to fountains developing on horizontal wall, some modes disappeared while others are split in several modes. This paper aims at describing and mapping these new modes regarding to the inclination and the inlet velocity. Explanations about what made the unstable modes evolve are also proposed.

RÉSUMÉ

Des expériences ont été menées sur des fontaines inversées faibles laminaires inclinées qui permettent d'assurer que les modes instables des fontaines circulaires sont perturbés par l'inclinaison. En effet, en comparant aux fontaines se développant sur paroi horizontale, certains modes disparaissent alors que d'autres se séparent en plusieurs modes. Ce papier a pour but de décrire et cerner ces nouveaux modes en fonction de l'inclinaison et de la vitesse d'injection. Des explications concernant l'origine de l'évolution des instabilités sont également proposées.

1. Introduction

A fountain refers to a flow generated by the injection of a buoyant fluid into a quiescent environment when the source momentum opposes the buoyancy. The development of this kind of flow can be described as follows: the momentum is acting first allowing the flow to rise while it entrains ambient fluid. Then the viscosity and the buoyant force reduces the flow momentum, forcing the flow to fall around the fountain core and lowering the maximum height which was first reached by the flow.

Fountains have been investigated by numerous authors [1–4] to characterize the fountain height or the unsteadiness of the flow which often leads to height oscillations [2]. Thanks to dimensional arguments, Turner [1] obtained the fountain height H_m as a function of the initial momentum flux $M_0 = \pi D^2 u^2/4$ and the initial buoyancy flux $F_0 = \pi g \Delta\rho D^2 u/4\rho$, assuming this height scales on the initial momentum jet length [5,6]:

$$H_m \sim M_0^{3/4} F_0^{-1/2} \tag{1}$$

* Corresponding author.
E-mail addresses: aymeric.lamorlette@yahoo.fr (A. Lamorlette), rabahpo@live.fr (R. Mehaddi), olivier.vauquelin@univmed.fr (O. Vauquelin).

1631-0721/$ – see front matter
doi:10.1016/j.crme.2011.01.004

where u refers to the vertical initial velocity, g the gravity, D the diameter of the injection, $\Delta\rho$ the initial density difference and ρ the ambient fluid density. This can be re-written as a function of the initial Froude number (based on the injection diameter) $Fr_D = u/\sqrt{gD\Delta\rho/\rho}$:

$$\frac{H_m}{D} \sim Fr_D = C_m Fr_D \tag{2}$$

Morton [5] found out that the constant C_m has a value which can be estimated as: $C_m = 3.48$ for the experiments he made on turbulent fountains in the range $1.5 < Fr_D < 21.2$ (as the Froude number definitions used can be slightly different from one author to another, the ranges given in this paper were shifted in order to match our Froude number definition).

Further studies where carried out on turbulent fountains, showing that the Reynolds number dependency can be neglected and that the fountain phenomenology remains the same as long as the initial flow is turbulent ($Re_D > 2000$ with $Re_D = uD/\nu$).

It can now be interesting to study if the correlation (and then the phenomenology) still stands for transient fountains ($200 < Re_D < 3000$) and for weak fountains ($Fr_D < 2.1$). A study by Zhang and Baddour [3] in the range $0.25 < Fr_D < 25$ allows to classify the fountains into two different regions, depending on the Froude number value. Indeed the usual correlation stands for $Fr_D > 4.9$. However, the fitting of the dimensionless height H_m/D is better using $H_m/D \sim Fr_D^{1.3}$ for $Fr_D < 4.9$, showing a different phenomenology. Another study by Kaye and Hunt [4] in the range $0.14 < Fr_D < 10.4$ shows a result which is not consistent regarding to those obtained by Zhang and Baddour [3]. Indeed, they now classified fountains in three different regions regarding to the dimensionless height fitting:

- forced fountains ($Fr_D > 2.1$): the fountains firstly described by Turner;
- weak fountains ($0.7 < Fr_D < 2.1$);
- very weak fountains ($Fr_D < 0.7$).

These regions have boundaries which are different from those found by Zhang and Baddour. The consistency problem emphasis by these results is most probably caused by the Reynolds number dependency. Indeed, Lin and Armfield [7] while studying intermediate Froude and Reynolds numbers fountains found out that for transient zones, the Froude number is not sufficient anymore to characterize a fountain. The introduction of a Reynolds number dependency has to be done. They empirically demonstrate that fountains were viscosity affected in the range $0.7 < Fr_D < 5.65$, $200 < Re_D < 1600$.

In order to clearly enlighten the role of the Reynolds and Froude numbers on fountains behaviour, Williamson et al. [8] studied fountains phenomenology in a large range of Froude and Reynolds numbers ($0.5 < Fr_D < 70.7$; $30 < Re_D < 3800$). In order to fit the description which has been done by Williamson et al., the whole problem will now be define using Froude and Reynolds numbers definition based on the injection radius r instead of the injection diameter (i.e. $Re = ur/\nu$ instead of $Re_D = uD/\nu$) so that $Re_D = 2Re$ and $Fr = \sqrt{2}Fr_D$.

The first behaviour of weak fountains to be observed is the steady one where the maximum penetration height is located on the fountain axis. When the fountain starts to be disturbed, the flapping/circling mode appears. This corresponds to a mode where the maximum penetration height is either flapping from one side to another of a plane rotating around the fountain axis, either circling around the fountain axis. The next behaviour to be observed is called flapping/bobbing. It refers to a situation where the fountain is either bobbing on the fountain axis, forcing the fountain to collapse from time to time, either flapping/circling as it was previously described. These three behaviours can be mapped on a Froude–Reynolds plane. The steady behaviour is to be observed in the range $0 < Fr < 16Re^{-2/3}$, the flapping/circling behaviour in the range $16Re^{-2/3} < Fr < 27Re^{-2/3}$ and the flapping/bobbing behaviour in the range $27Re^{-2/3} < Fr < 35Re^{-2/3}$.

Williamson et al. also demonstrate that miscible fountains exhibit height fluctuation frequencies which are similar to those observed by Clanet [9] for non-miscible fountains. Lin and Armfield [10] show that the miscible behaviour of laminar and transient fountains does not modify the correlation on the fountain height. The phenomenology of weak laminar fountains should then be similar for miscible and non-miscible fountains.

Now that the different fountains observed at low Reynolds–Froude numbers are well-described (the high Reynolds–Froude numbers fountains study falls outside the scope of this article), the effect of an inclination can be studied for these flows. Previous works were intended on inclined jets and plumes. A study on inclined fountains by Bloomfield et al. [11] focus on the evolution of the fountain height regarding to the inclination. This study however has been conducted using a salient injection, the phenomenology then cannot be compared.

An experimental apparatus similar to the one used by Williamson et al. (non-salient injection in a large open chamber or on a plane where sides are free so that the injected fluid can flow everywhere without accumulation) has to be used in order to show the effect of an inclination on the fountain behaviour.

2. Experimental apparatus

The experiments are carried out on a 1 m × 2 m wood plane hanging on a frame so that the fluid can freely flow outside the plane. The frame allows the plane to be inclined within the range $2.5° < \gamma < 15°$. Experiments are conducted on reversed fountains so that the "heavy" fluid is the ambient air ($\rho = 1.22\ \mathrm{kg\,m^{-3}}$) and the downward injected "light" fluid is either pure helium ($\rho = 0.17\ \mathrm{kg\,m^{-3}}$) or a helium–air mix ($Y_{He} = Y_{air} = 0.5$) with ammonium salts as dye. The helium

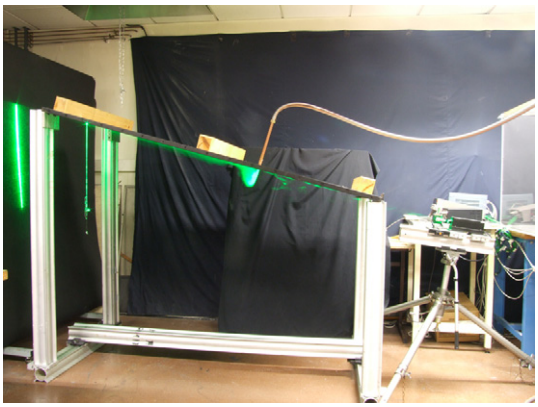

Fig. 1. Experimental setup.

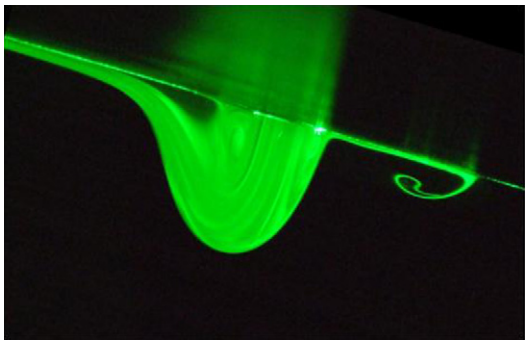

(a) Viewing perpendicular to the wood plane in the direction of steepest ascent

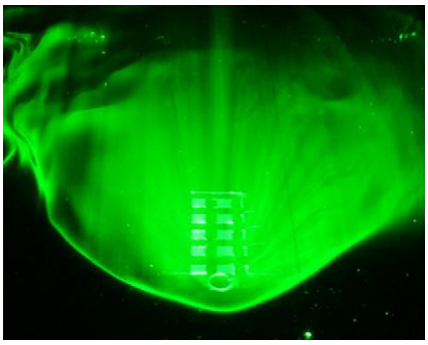

(b) Viewing parallel to the wood plane

Fig. 2. Steady fountain, $\gamma = 12°$.

(or helium–air) flow is controlled using an Aalborg flowmeter able to supply up to 50 l/mn of helium (the accuracy of the flowmeter is 0.1 l/mn for both air and helium). This flowmeter is also mixing air with helium when the helium–air mix is used. The helium is injected by a perpendicular non-salient 15 mm diameter 450 mm long copper pipe. This apparatus can supply a flow within the following ranges: $37 < Re < 128$ and $1.7 < Fr < 7.5$ for pure helium and $50 < Re < 169$ and $0.9 < Fr < 3.0$ for the helium–air mix. It assures that a laminar flow is fully developed when it reaches the outlet of the pipe.

Now that the range of Reynolds and Froude numbers is defined for our experiments, the diffusion has to be investigated. The Peclet number $Pe = ReSc$ (with $Sc = \nu/D_m$, D_m being the mass diffusivity) is in the range [100; 1000]. It assess that an analogy is possible between the miscible fountains which are studied here and non-miscible fountains. Indeed, the flow phenomenology is here mainly characterized on small time periods near the injection, so that diffusion can be neglected.

The fountain is then lit by a 2 Watt monochromatic LASER plane either perpendicular to the wood plane in the direction of steepest ascent either parallel to the wood plane. Pictures of the flows were taken using either a Fujifilm Finepix 9001 camera, either a PCO 1200 hs high speed camera with a 50 mm Nikon lens. The cameras setup is always done to lower saturation and provides sharp pictures; the exposure time is around 5×10^{-3} s. A picture of the experimental setup is shown in Fig. 1.

3. Flow description

The three main flows observed at low Froude–Reynolds number are now going to be described. The first one is the steady one which is observed for every angle value in the range $2.5° < \gamma < 15°$ for low inlet velocities. An annular vortex appears around the injection with an asymmetry (the higher are the velocity and the angle, the stronger is the asymmetry). Indeed the vortex in the upward part of the flow is higher but smaller in length as in the downward part. The light fluid is flowing down this vortex radially, mostly downward creating a gravity current but some of the helium flows down upward. This part of the flow is slowed down by the radial expansion, lowering its momentum until buoyant forces make it flow downward over and along the first gravity current. This flow is illustrated in Figs. 2(a) and 2(b).

When the velocity starts to increase, two different behaviours can occur depending on the inclination, but the phenomenon that breaks the steadiness of the fountain is the same in both cases. Indeed, whatever is the angle, when the upward part of the vortex starts being too high, the gravity current that flows over it is not strong enough to prevent the

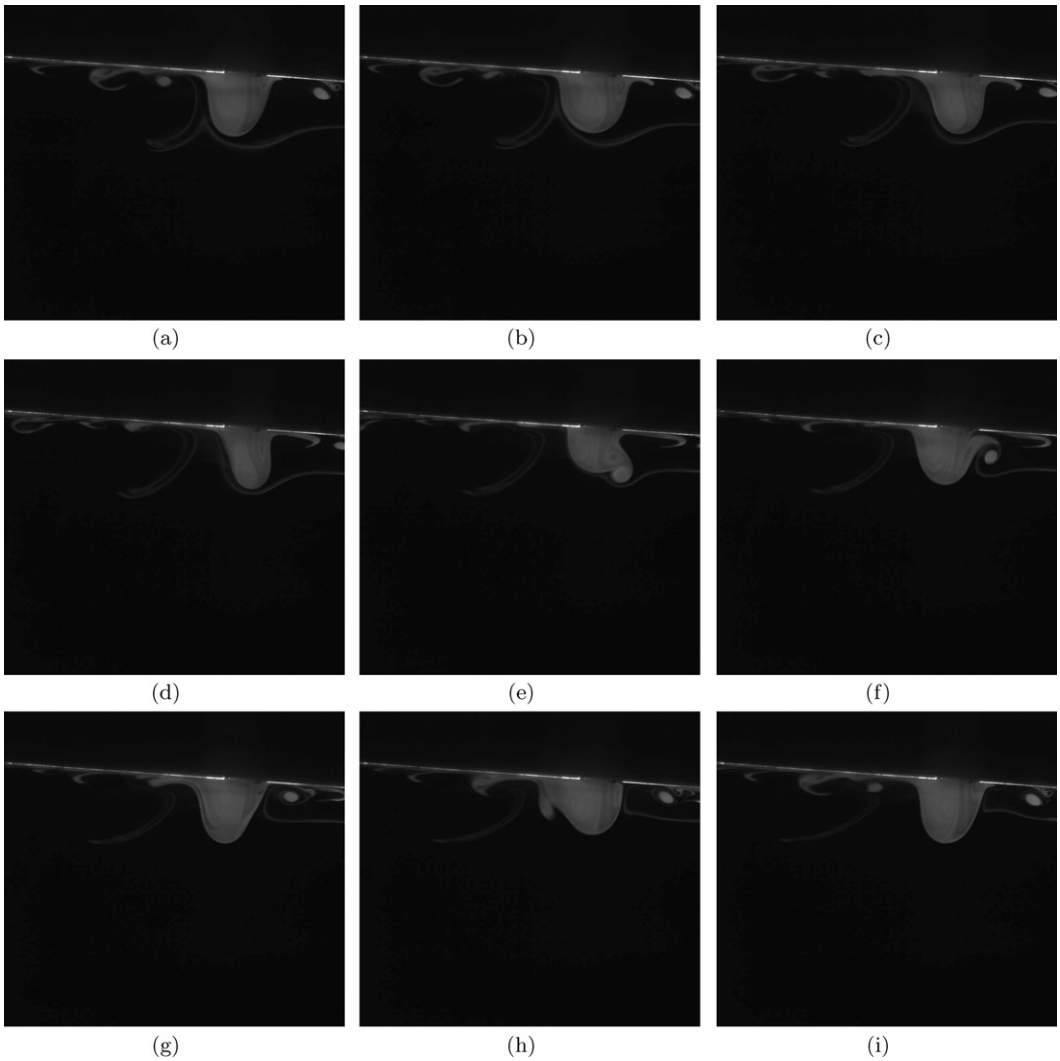

Fig. 3. Sequence of the alternate bobbing, $\gamma = 2.5°$, $Fr = 3.2$, $Re = 51$.

buoyant forces of the vortex from stretching it in the vertical direction, forcing around half of the upward part of the vortex to separate and flow over the fountain in a crescent-shaped vortex; the remaining of the upward part of the vortex is then reforming a whole vortex with the downward part of the vortex. A part of the upward flow is then bobbing before it flows downward.

If the angle is weak, the matter that flows in the crescent-shaped vortex forces the downward part of the vortex to rise upward. This process is stretching the downward part of the vortex vertically, forcing it to separate into two parts as it happened to the upward part. The downward flow is bobbing and then flowing upward, causing the process to repeat itself. This fountain mode is called alternate bobbing. A 0.5 second sequence showing the whole process is presented in Fig. 3 for $\gamma = 2.5°$, $Fr = 3.2$ and $Re = 51$ from left to right and from top to bottom (the last picture is the same as the first one). The time step between each picture is regular, the vortex shedding frequency is 2 Hz.

In the downward part of the flow, the global shape of the gravity current generated by the fountain is kept (when compared with the steady case). However small discontinuities are to be observed where the vortex has been pulled out (where a part of the vortex is pulled out, the gravity current is locally detached). Eddies generated by the bobbing process are also running over the gravity current, being stretched by it while convected (the gravity current is quicker than the eddies ejected over it; it is also spreading radially, causing the eddies to be stretched forward and radially). In the upward part of the flow, the behaviour is a bit different. Indeed, as in the steady case, the gravity current is slowed down by the radial expansion and the buoyant forces before it flows downward over and along the first gravity current. This cause the discontinuities and the eddies to collapse on themselves, creating a single eddy at the rear of the flow. This flow is illustrated in Fig. 5(a).

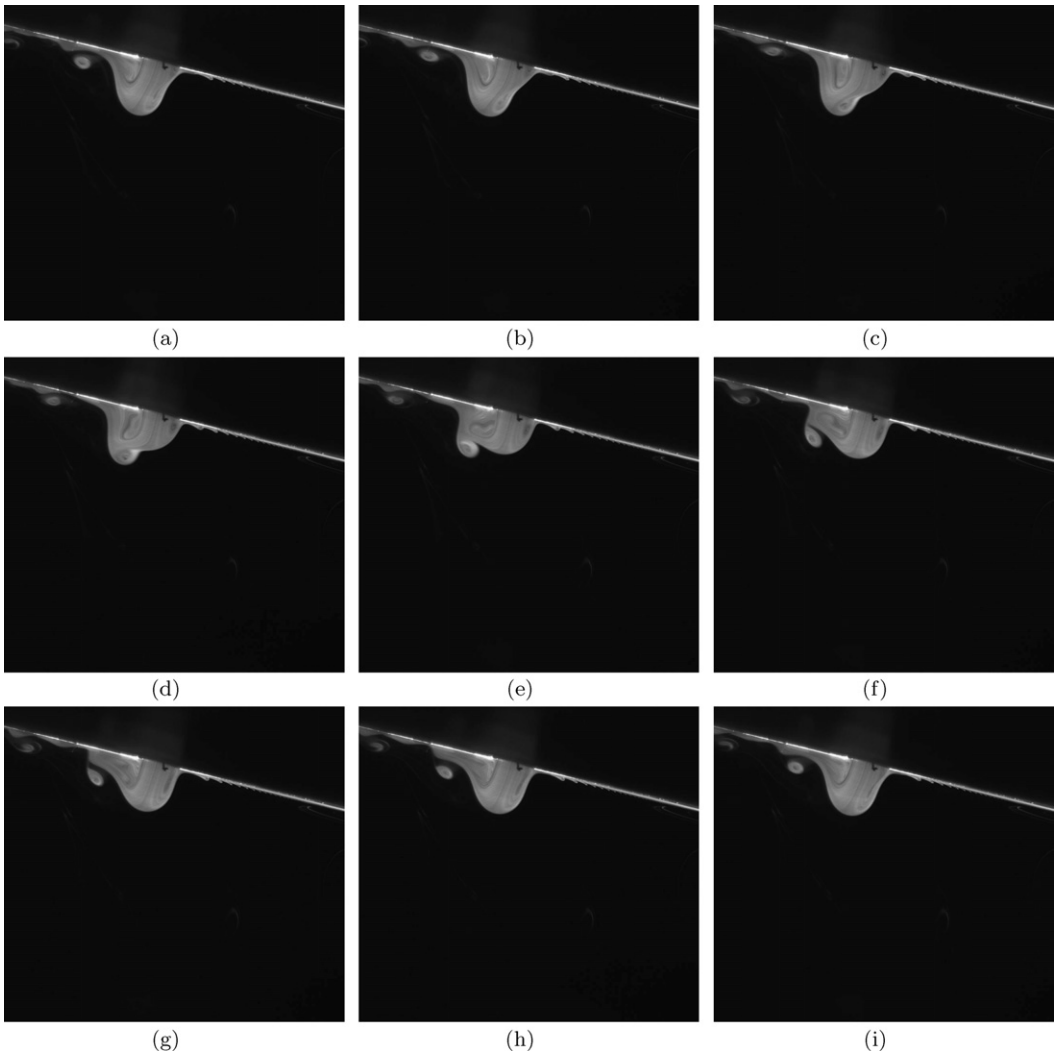

Fig. 4. Sequence of the forward bobbing, $\gamma = 12^\circ$, $Fr = 2.9$, $Re = 46$.

If the angle is important, the matter that flows in the crescent-shaped vortex cannot force the downward part of the vortex to rise upward as its buoyancy is too strong to let it go: the downward part of the vortex is stretched but not enough to be broken so it just reforms itself once the crescent-shaped vortex flowed over it. The situation is then the same as when the upward part of the vortex started being too high: a part of the upward part of the vortex is bobbing before it flows downward. The process repeats itself creating a forward bobbing. A 0.12 second sequence showing the whole process is presented in Fig. 4 for $\gamma = 12^\circ$, $Fr = 2.9$ and $Re = 46$ from left to right and from top to bottom (the last picture is again the same as the first one). The time step between each picture is regular, the vortex shedding frequency is 8.33 Hz.

The downward gravity current exhibits the same features as those observed in the alternate bobbing case (eddies spreading forward and radially) without discontinuities (the downward part of the vortex is never pulled out in this case so that the downward gravity currents cannot shows any discontinuity). The upward gravity current is however discontinuous (without eddies) as the upward part of the vortex is regularly pulled out so that a single eddy formed by the collapsing of the discontinuities can be observed at the rear of the flow. This rear eddy is located nearer from the injection than in the alternate bobbing case as less momentum is going upward in this case. This flow is illustrated in Fig. 5(b).

4. Discussion

Fig. 6 shows a mapping of the three presented modes in the spaces $\{u; \gamma\}$. The limits between fountain modes are obtained by setting the angle to a given value before making the inlet velocity rise, starting with a steady fountain. When the steady-state is broken the critical velocity is reached, giving either the limit between steady and alternate bobbing either the limit between steady and forward bobbing.

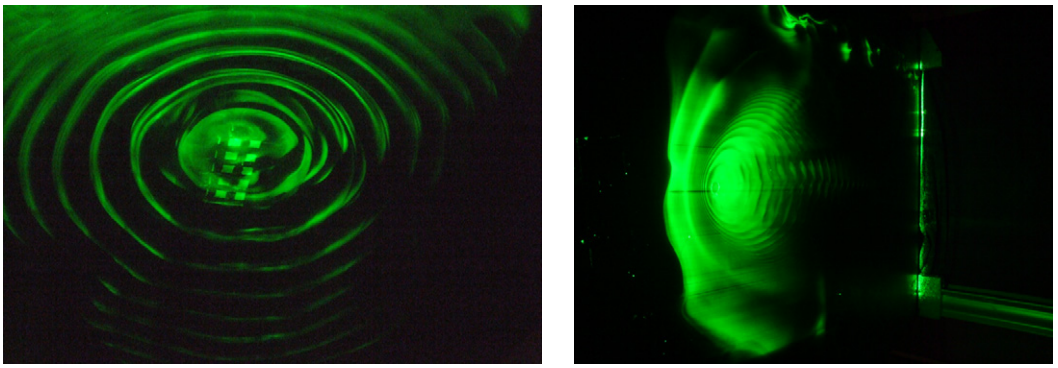

(a) Alternate bobbing, $\gamma = 2.5°$, $Fr = 3.2$, $Re = 51$ (b) Forward bobbing, $\gamma = 12°$, $Fr = 2.9$, $Re = 46$

Fig. 5. Alternate and forward bobbing, viewed parallel to the plane.

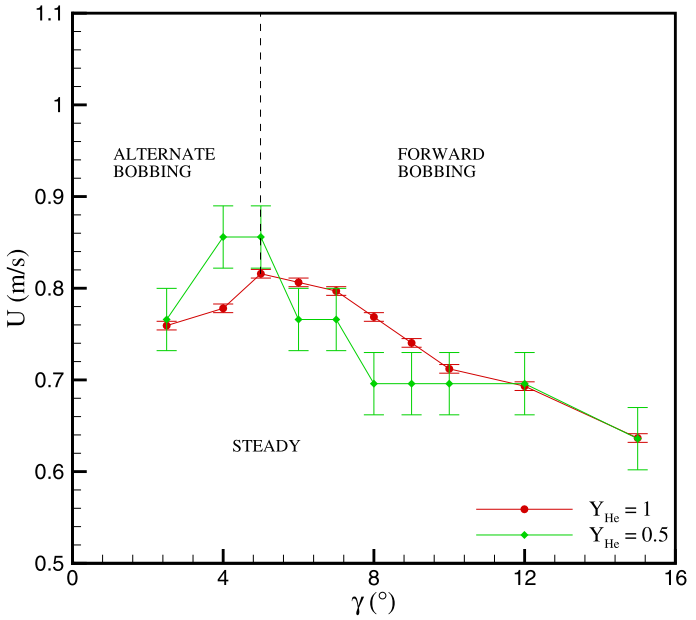

Fig. 6. Mapping of the inclined fountain modes in the spaces $\{u; \gamma\}$.

At first, it can be noticed that the critical angle $\gamma_{cr} = 5°$ for which the unstable fountain mode changes is the same for both helium concentrations.

Other features are to be enlighten which are consequences of the inclination. Indeed, the inclination is breaking the steady fountain symmetries (as the vortex surrounding the injection is asymmetric, the whole fountain is asymmetric). If the steady fountain has less symmetries it becomes more stable, the steady-state will stand in a larger Froude–Reynolds range.

As the inclination creates a preferred direction for instabilities, the flapping/circling mode described by Williamson cannot exist anymore when the fountain is inclined. The classical bobbing described by Williamson with a fountain top collapsing on itself also cannot stand because of the inclination. These two modes are replaced by a new bobbing process split into two modes regarding the inclination angle.

The global consequence is that the steady-state is stabilized by the inclination until it reaches the limit $\gamma_{cr} = 5°$ (the higher is the angle, the better is the stabilization). The inclination then destabilizes the steady-state (if the angle becomes more important, the bobbing can occur at lower inlet velocities because the buoyant forces of the upward part of the vortex are strongly acting to destabilize it). The angle is then firstly stabilizing the fountain before it destabilizes it, forcing the classical bobbing to be split into two different modes.

Finally, other modes were observed for higher values of the inlet velocity which are different from those described by Williamson (again, because of the inclination which creates a preferred direction for instabilities), but they were not easy to catch with a great accuracy. This study should then be expanded on a larger range of inlet velocities and diameter so that the mapping of inclined fountains behaviour can be presented in terms of Reynolds–Froude angle dependency.

References

[1] J.S. Turner, Jets and plumes with negative or reversing buoyancy, J. Fluid Mech. 26 (4) (1966) 779–792.
[2] E. Villermaux, Pulsed dynamics of fountains, Nature 371 (1994) 24–25.
[3] H. Zhang, R.E. Baddour, Maximum penetration of vertical round dense jets at small and large Froude numbers, J. Hydraul. Engng. 124 (1998) 550–553.
[4] N.B. Kaye, G.R. Hunt, Weak fountains, J. Fluid Mech. 558 (2006) 319–328.
[5] B.R. Morton, G.I. Taylor, J.S. Turner, Turbulent gravitational convection from maintained and instantaneous sources, Proc. R. Soc. London Ser. A 234 (1) (1956).
[6] B.R. Morton, Forced plumes, J. Fluid Mech. 5 (1) (1959) 151–163.
[7] W. Lin, S.W. Armfield, Direct numerical simulation of fountains with intermediate Froude and Reynolds numbers, ANZIAM J. 45 (2004) 66–77.
[8] N. Williamson, N. Srinarayana, S.W. Armfield, G.D. McBain, W. Lin, Low-Reynolds-number fountain behaviour, J. Fluid Mech. 608 (2008) 297–317.
[9] C. Clanet, On large-amplitude pulsating fountains, J. Fluid Mech. 366 (1998) 333–350.
[10] W. Lin, S.W. Armfield, The Reynolds and Prandtl number dependence of weak fountains, Comput. Mech. 31 (2003) 379–389.
[11] L.J. Bloomfield, R.C. Kerr, Inclined turbulent fountains, J. Fluid Mech. 451 (2002) 283–294.